

Long-term passage impacts human dental pulp stem cell activities and cell response to drug addition *in vitro* (#100444)

1

First submission

Guidance from your Editor

Please submit by **3 Jul 2024** for the benefit of the authors (and your token reward) .



Structure and Criteria

Please read the 'Structure and Criteria' page for guidance.



Custom checks

Make sure you include the custom checks shown below, in your review.



Raw data check

Review the raw data.



Image check

Check that figures and images have not been inappropriately manipulated.

If this article is published your review will be made public. You can choose whether to sign your review. If uploading a PDF please remove any identifiable information (if you want to remain anonymous).

Files

Download and review all files from the [materials page](#).

10 Figure file(s)

1 Raw data file(s)



Custom checks

Cell line checks



Is the correct provenance of the cell line described?




Structure and Criteria

Structure your review

The review form is divided into 5 sections. Please consider these when composing your review:

1. **BASIC REPORTING**
2. **EXPERIMENTAL DESIGN**
3. **VALIDITY OF THE FINDINGS**
4. General comments
5. Confidential notes to the editor






 You can also annotate this PDF and upload it as part of your review

When ready [submit online](#).





Editorial Criteria

Use these criteria points to structure your review. The full detailed editorial criteria is on your [guidance page](#).




BASIC REPORTING

-  Clear, unambiguous, professional English language used throughout.
-  Intro & background to show context. Literature well referenced & relevant.
-  Structure conforms to [Peerj standards](#), discipline norm, or improved for clarity.
-  Figures are relevant, high quality, well labelled & described.
-  Raw data supplied (see [Peerj policy](#)).

EXPERIMENTAL DESIGN

-  Original primary research within [Scope of the journal](#).
-  Research question well defined, relevant & meaningful. It is stated how the research fills an identified knowledge gap.
-  Rigorous investigation performed to a high technical & ethical standard.
-  Methods described with sufficient detail & information to replicate.

VALIDITY OF THE FINDINGS

-  **Impact and novelty is not assessed.** Meaningful replication encouraged where rationale & benefit to literature is clearly stated.
-  All underlying data have been provided; they are robust, statistically sound, & controlled.
-  Conclusions are well stated, linked to original research question & limited to supporting results.



The best reviewers use these techniques

Tip

Example

Support criticisms with evidence from the text or from other sources

Smith et al (J of Methodology, 2005, V3, pp 123) have shown that the analysis you use in Lines 241-250 is not the most appropriate for this situation. Please explain why you used this method.

Give specific suggestions on how to improve the manuscript

Your introduction needs more detail. I suggest that you improve the description at lines 57- 86 to provide more justification for your study (specifically, you should expand upon the knowledge gap being filled).

Comment on language and grammar issues

The English language should be improved to ensure that an international audience can clearly understand your text. Some examples where the language could be improved include lines 23, 77, 121, 128 – the current phrasing makes comprehension difficult. I suggest you have a colleague who is proficient in English and familiar with the subject matter review your manuscript, or contact a professional editing service.

Organize by importance of the issues, and number your points

1. Your most important issue
2. The next most important item
3. ...
4. The least important points

Please provide constructive criticism, and avoid personal opinions

I thank you for providing the raw data, however your supplemental files need more descriptive metadata identifiers to be useful to future readers. Although your results are compelling, the data analysis should be improved in the following ways: AA, BB, CC

Comment on strengths (as well as weaknesses) of the manuscript

I commend the authors for their extensive data set, compiled over many years of detailed fieldwork. In addition, the manuscript is clearly written in professional, unambiguous language. If there is a weakness, it is in the statistical analysis (as I have noted above) which should be improved upon before Acceptance.

Long-term passage impacts human dental pulp stem cell activities and cell response to drug addition *in vitro*.

Somying Patntirapong^{Corresp., 1}, Juthaluck Khankhow², Sikarin Julamorn²

¹ Thammasat University Research Unit in Dental and Bone Substitute Biomaterials, Faculty of Dentistry, Thammasat University, Pathumthani, Thailand

² Faculty of Dentistry, Thammasat University, Pathumthani, Thailand

Corresponding Author: Somying Patntirapong
Email address: psomying@tu.ac.th

Background: Dental pulp stem cells (DPSCs) possess mesenchymal stem cell characteristics and have potential for cell-based therapy. Cell expansion is essential to achieve sufficient cell numbers. However, continuous cell replication causes cell aging *in vitro*, which usually accompanies and potentially affect DPSC characteristics and activities. Continuous passaging could alter susceptibility to external factors such as drug treatment. Therefore, this study sought to investigate potential outcome of *in vitro* passaging on DPSC morphology and activities in the absence or presence of external factor. **Methods:** Human DPSCs were subcultured until reaching early passages (P5), extended passages (P10), and late passages (P15). Cells were evaluated and compared for cell and nuclear morphologies, cell adhesion, proliferative capacity, alkaline phosphatase (ALP) activity, and gene expressions in the absence or presence of external factor. Alendronate (ALN) drug treatment was used as an external factor. **Results:** Continuous passaging of DPSCs gradually lost their normal spindle shape and increased in cell and nuclear sizes. DPSCs were vulnerable to ALN. The size and shape were altered, leading to morphological abnormality and inhomogeneity. Long-term culture and ALN interfered with cell adhesion. DPSCs were able to proliferate irrespective of cell passages but the rate of cell proliferation in late passages was slower. ALN at moderate dose inhibited cell growth. ALN caused reduction of ALP activity in early passage. In contrast, extended passage responded differently to ALN by increasing ALP activity. Late passage showed higher collagen but lower osteocalcin gene expressions compared with early passage in the presence of ALN. **Conclusion:** An increase in passage number played critical role in cell morphology and activities as well as responses to the addition of an external factor. The effects of cell passage should be considered when used in basic science research and clinical applications.

Title:

Long-term passage impacts human dental pulp stem cell activities and cell response to drug addition *in vitro*.

Running title:

Culture and alendronate affect pulp cell.

Author: Somying Patntirapong^{1,*}, Juthaluck Khankhow², Sikarin Julamorn²

Affiliation:

¹Thammasat University Research Unit in Dental and Bone Substitute Biomaterials, Faculty of Dentistry, Thammasat University, Pathumthani, Thailand

²Faculty of Dentistry, Thammasat University, Pathumthani, Thailand

***Corresponding author:**

Somying Patntirapong

Faculty of Dentistry, Thammasat University, Rangsit campus

99 Moo 18 Pahonyothin Rd., Klong Luang,

Pathumthani, 12120, Thailand

E-mail address: psomying@tu.ac.th; p_somying@hotmail.com

24 Abstract

25 **Background:** Dental pulp stem cells (DPSCs) possess mesenchymal stem cell characteristics
 26 and have potential for cell-based therapy. Cell expansion is essential to achieve sufficient cell
 27 numbers. However, continuous cell replication causes cell aging *in vitro*, which usually
 28 accompanies and potentially affect DPSC characteristics and activities. Continuous passaging
 29 could alter susceptibility to external factors such as drug treatment. Therefore, this study sought
 30 to investigate potential outcome of *in vitro* passaging on DPSC morphology and activities in the
 31 absence or presence of external factor.

32 **Methods:** Human DPSCs were subcultured until reaching early passages (P5), extended
 33 passages (P10), and late passages (P15). Cells were evaluated and compared for cell and nuclear
 34 morphologies, cell adhesion, proliferative capacity, alkaline phosphatase (ALP) activity, and
 35 gene expressions in the absence or presence of external factor. Alendronate (ALN) drug
 36 treatment was used as an external factor.

37 **Results:** Continuous passaging of DPSCs gradually lost their normal spindle shape and increased
 38 in cell and nuclear sizes. DPSCs were vulnerable to ALN. The size and shape were altered,
 39 leading to morphological abnormality and inhomogeneity. Long-term culture and ALN
 40 interfered with cell adhesion. DPSCs were able to proliferate irrespective of cell passages but the
 41 rate of cell proliferation in late passages was slower. ALN at moderate dose inhibited cell
 42 growth. ALN caused reduction of ALP activity in early passage. In contrast, extended passage
 43 responded differently to ALN by increasing ALP activity. Late passage showed higher collagen
 44 but lower osteocalcin gene expressions compared with early passage in the presence of ALN.

Conclusion: An increase in passage number played critical role in cell morphology and activities as well as responses to the addition of an external factor. The effects of cell passage should be considered when used in basic science research and clinical applications.

Keywords: Cell passage; alendronate; cell morphology; nuclear morphology; proliferation; alkaline phosphatase activity

Introduction

Mesenchymal stem cells (MSCs) are multipotent cells, capable of giving rise to many cell lineages. Although MSCs were primarily identified in the bone marrow, they can be isolated from tissues in the oral cavity. Human dental pulp stem cells (DPSCs) are post-natal populations of MSCs residing in the pulp cavity of permanent teeth (Gronthos, Mankani et al. 2000). DPSCs are considered feasible and promising source of autologous stem cells because they have MSC qualities (Gronthos, Mankani et al. 2000, Huang, Gronthos et al. 2009, Awais, Balouch et al. 2020) and are cost-effective. Their isolation procedure is less invasive and can be obtained from discarded or removed teeth such as premolar and third molar. Isolated *ex vivo* DPSCs are characterized as cells with a high level of clonogenicity and proliferation and share a similar immunophenotype to that of bone marrow MSCs *in vitro* (Gronthos, Mankani et al. 2000). DPSCs, when placed under specific conditions, generate different cell lineages: odonto/osteogenic, chondrogenic, neurogenic, adipogenic, and myogenic (Huang, Gronthos et al. 2009, Mangano, Paino et al. 2011, Kogo, Seto et al. 2020). These cells are capable of forming mineralized nodule *in vitro* and regenerate a dentin-like structure *in vivo* (Gronthos, Mankani et al. 2000).

Human stem cells can easily be cultivated, expanded, and cryopreserved as well as produce progeny with strong differentiation capacity. Therefore, use of these cells has become common for many purposes ranged from scientific studies to tissue engineering in order to replace damaged cells using autologous transplant in various diseases. DPSCs have also been increasingly studied and employed in regenerative field including cell-guided regeneration for correcting of bone defects (d'Aquino, De Rosa et al. 2009, Mangano, Paino et al. 2011, Awais, Balouch et al. 2020).

MSC-based therapies and studies demand large scale *ex vivo*/*in vitro* expansion to reach the numbers required for cell therapy. Cell deterioration after prolonged expansion in cell culture is an unavoidable physiological consequence (Hayflick and Moorhead 1961). Late cell passages affect cell appearance, proliferative capability, and osteogenic differentiation (Yang, Ogando et al. 2018, Grotheer, Skrynecki et al. 2021). MSCs gradually lose their typical fibroblast shape and lack morphological homogeneity (Yang, Ogando et al. 2018). The rate of cell doublings significantly decreases (Yang, Ogando et al. 2018), which are not suitable for therapeutic application. DPSCs undergoing many serial passaging also display a reduction in cell proliferation and viability (Martin-Piedra, Garzon et al. 2014, Yan, Nada et al. 2022). *In vivo* transplantation of DPSCs demonstrates a restriction in the differentiation capacity into osteoblast lineage at high passage (9th) (Yu, He et al. 2010). Cell adhesion and spreading are crucial for cell proliferation, differentiation, and mineralization (Simon, Cohen-Bouhacina et al. 2003). Thus, the success of cell attachment and interaction with the surface of the substrates depend on these activities. Nevertheless, these cellular aspects as well as cell morphology of long-term cultivated DPSCs are still unclear.

DPSCs have ability to respond to several influences such as caries and other biochemical and mechanical factors. DPSCs respond to high dose of lipopolysaccharide by increase in cell death (Gao, You et al. 2020). On the other hand, *ex vivo* DPSCs exposure to deep caries still have proliferative capability and express higher angiogenic marker (Chen, Li et al. 2021). Activation of K⁺ channels in DPSCs induces the differentiation of DPSCs into neuron-like cells (Kogo, Seto et al. 2020). Long-term expansion could be an influence on cell response to an external factor/chemical factor/inciting factor. Due to the lack of this information, it was thus essential to determine the influence of *in vitro* passaging on cellular qualities under an external

condition. Therefore, the present work sought to investigate 1) DPSC activities at different passages to determine the optimal passage and 2) cell activities at different passages in the present of external factor. Alendronate (ALN) is an anti-resorptive drug, which is known to have inhibitory effects on osteoblasts (Patntirapong, Singhatanadgit et al. 2014, Patntirapong, Korjai et al. 2021). In this study, ALN drug treatment was served as an external factor added to DPSC culture. Long-term DPSC subcultures from passage 5-15 under ALN-free and ALN conditions were evaluated for cell adhesion, cell morphology, cell proliferation, and alkaline phosphatase activity.

Materials and methods

Cell culture and treatments

The manuscript of this laboratory study has been written according to Preferred Reporting Items for Laboratory studies in Endodontology (PRILE) 2021 guidelines. Human DPSCs (PT-5025) were obtained from Lonza (Walkersville, Inc). According to the company's data, DPSCs are tested for CD105⁺, CD166⁺, CD29⁺, CD90⁺, CD73⁺, CD133⁻, CD34⁻, CD45⁻ using flow cytometry. Cells were continuously passaged until reaching passage 16. Cell passage 4-6, 9-11, and 14-16 were used in the experiments and these passages were referred to as P5 (early passage), P10 (extended passage), and P15 (late passage), respectively. DPSCs were maintained in standard culture media, which were Dulbecco's modified Eagle's medium (DMEM, Gibco) supplement with 10% fetal bovine serum and 1% penicillin/streptomycin at 37°C and 5% CO₂ humidified atmosphere. DPSCs were plated at the density of 7,500 cells/cm² and then treated with ALN at various concentrations (0, 0.1, 0.5, 5, 10 μM). In this study, 0.1-0.5 μM ALN was considered low concentration and 5-10 μM ALN was moderate concentration. For

cell differentiation, DPSCs were cultured under osteogenic media (OM), which were standard culture media supplemented with 50 µg/ml ascorbic acid (BDH), 10 mM β-glycerophosphate (Sigma), and 100 nM dexamethasone.

Cell adhesion assay

Cells were seeded and treated with ALN for 5 hours. Non-adherent cells were removed by gently washing with phosphate-buffered saline solution. Adherent cells were fixed with 4% paraformaldehyde for 15 minutes at room temperature. Cells were stained with 1% crystal violet (Reag. Ph. Eur.) for 20 minutes and rinsed carefully. Cells were examined under a microscope (Nikon Eclipse Ti, Nikon Instruments) at 100x magnification. Ninety-six images of cells from four wells were captured using NIS element AR 4.11.00 software. The numbers of cells ranged from 190-2084 were recorded and analyzed.

Cell and nuclear morphological assay

Cells were treated with ALN for 3 days. Cells were fixed with 4% paraformaldehyde for 15 minutes and incubated with 1% crystal violet for 20 minutes. Cell appearance was monitored at 100x magnification. Forty areas from four wells were recorded and 410-600 cells were analyzed. Nuclear shape was stained with 4',6-diamidino-2-phenylindole (DAPI) at the dilution 1:1000 for 5 minutes. Nuclei were visualized under a confocal microscope (Nikon Eclipse Ti, Nikon Instruments) at 200x magnification. The numbers of nuclei ranged from 447-675 were examined.

Image analysis

Quantitative data was analyzed by ImageJ software version 1.53k Java 1.8.0 (National Institute of Health). Images of cells stained with crystal violet were assessed according to previous report (Patntirapong, Charoensukpatana et al. 2022). In brief, the scale was set in a micrometer unit. Original images were processed by automated detection mode. The background of images was eliminated using Subtract Background function. Images were converted to 8-bit grayscale and were processed by Auto Threshold commands. Cluster cells were optionally segmented by Watershed function. Cells were identified and analyzed by Analyze Particles function. Data from isolated cells were collected. In the cell morphological test, the particles smaller than $200\ \mu\text{m}^2$ were excluded and identified as debris. For nuclear analysis, images of the nuclei were processed as described in previous report (Patntirapong, Chanruangvanit et al. 2021). Quantitative data such as area (μm^2), perimeter (μm), roundness, aspect ratio (AR), circularity, solidity, and number were measured.

Cell proliferation assay

DPSCs treated for 1, 3, and 7 days were incubated with $10\ \mu\text{L}$ of the CCK-8 solution (Dojindo Laboratories) at 37°C for 3 hours according to company instruction. The plates were analyzed using a microplate reader (Sunrise) with Megellan software, V6.6 at the absorbance $450\ \text{nm}$.

Protein measurement and alkaline phosphatase (ALP) activity

Cells were cultured in OM and treated with ALN for 7 days. Media were collected for measuring ALP released in the media. Cells were lysed with Triton X-100 lysis buffer (50 mM Tris, 150 mM NaCl, and 1% Triton X-100, pH 10). Cell lysates were measured for total proteins

using the BCA protein assay kit (Pierce). The mixture was read at absorbance 562 nm using a microplate reader. Total protein was quantified against known BCA protein concentration. The aliquots with an equal amount of protein content from each sample and media were incubated with ALP substrate using ALP assay kit (Elabsience) at 37°C for 15 minutes. The optical density of p-nitrophenol was determined by a spectrophotometer at 520 nm. ALP activity was calculated relative to standard phenol solution and expressed as ng/ml.

Real-time polymerase chain reaction (PCR)

mRNA was isolated from OM-induced cells using the Total RNA Mini kit (Geneaid). All purified mRNA samples were processed into cDNA using oligo dT (TAKARA BIO INC.). cDNA samples were amplified in a reaction mix containing KAPA SYBR® FAST PCR Kit Master Mix (Thermo Fisher Science) and the forward and reverse primer pair sequences (Sigma). The amplification was run in QuantStudio™ 3 Real-Time PCR Systems (Thermo Fisher Scientific). The cycles were set at 50 °C for 2 min initial heating, 95 °C for 1 min, 40 cycles of 95 °C for 30 s, followed by 60 °C for 30 s with 72 °C elongation for 30 s. The forward/reverse primer pairs were as follows: glyceraldehyde 3-phosphate dehydrogenase (GAPDH) "CTCATTTTCCTGGTATGACACC" and "CTTCCTCCTGTGCTCTTGCT"; collagen type I (Col I) "TGACCTCAAGATGTGCCACT" and "ACCAGACATGCCTCTTGTCC"; osteocalcin (OC) "TCACACTCCTCGCCCTATTG" and "TCGCTGCCCTCCTGCTTG"; Bone sialoprotein (BSP) "AACCTACAACCCACACAA" and "AGGTTCCCCGTTCTCACTTT"; dentin sialophosphoprotein (DSPP) "AGACGAGGGTTCTGGTGATG" and "TCTTCTTTCCCATGGTCCTG"; dentin matrix acidic phosphoprotein 1 (DMP1) "GCAGAGTGATGACCCAGAG" and

“GCTCGCTTCTGTCATCTTCC”. The gene copy number was normalized with GAPDH. Data were presented in fold changes relative to control of each group.

Statistical analysis

Four independent experiments were performed. Data was tested for normal distribution using Kolmogorov-Smirnov test (GraphPad Prism 9.4.0). Data that was normally distributed was analyzed by ANOVA followed by Dunnett's test. Data that was not normally distributed was analyzed by Kruskal Wallis test followed by Dunn's procedure. Significance was assigned as * $p < 0.05$, ** $p < 0.01$, *** $p < 0.001$ vs P5 in the same ALN treatment group; ^a $p < 0.05$, ^{aa} $p < 0.01$, ^{aaa} $p < 0.001$ vs P5A0 in P5 group; ^b $p < 0.05$, ^{bb} $p < 0.01$, ^{bbb} $p < 0.001$ vs P10A0 in P10 group; ^c $p < 0.05$, ^{cc} $p < 0.01$, ^{ccc} $p < 0.001$ vs P15A0 in P15 group.

Results

Alteration of cell morphology in early, extended, and late passages under ALN-free and ALN conditions

Microscopic images of DPSCs at P5, P10, and P15 are depicted in Fig 1A, 1B, and 1C, respectively. Cells in each condition showed different cell size and shape. Untreated DPSCs at P5 were small in size and mainly spindle shape (Fig 1Ai), which mostly maintained the shape and size as observed in P1 cells (Fig 1D). Continuous culture led to morphological alteration. P10 and P15 cells gradually spread and appeared as polygonal shape. Cells displayed less homogenous morphologies. DPSCs at P15 noticeably exhibited enlarged cell bodies with extended cellular processes. Fewer cells were observed for P10 and P15 (Fig 1Bi and 1Ci). Addition of ALN to P5 cells altered the cell shape to fusiform (Fig 1Aiv) or polygonal with more

cellular processes (Fig 1Av). However, cell shrinkage from 10 μ M ALN (A10) was observed (Fig 1Av). Addition of A5 and A10 to P10 and P15 also altered cell shape (Fig 1B and 1C).

Cell area and perimeter of P10 and P15 were larger than those of P5 in ALN-free and ALN-treated groups (Fig 2A and 2B). Treatment with A10 increased cell area in every passage (Fig 2A). In P5, treatment with A0.1-A10 enhanced cell perimeter (Fig 2B).

Aspect ratio (AR) describes the proportional relationship between the width of a cell and its length. P10 in A0-A0.5 groups had lower AR but P10 in A5-A10 groups showed higher AR compared with P5. P5 treated with A0.5-A10 significantly different from P5A0, whereas P15 treated with A5 notably had higher AR than P15A0 (Fig 2C). Roundness demonstrated the opposite trend from AR (Fig 2D).

Circularity is a ratio of area and perimeter. The value of one means that the object has a circular shape. Solidity differentiates the convex and the concave cell area (Hart, Lauer et al. 2017). Alteration in circularity and solidity implies changes in cell deformability and cell shape (Pasqualato, Lei et al. 2013, Hart, Lauer et al. 2017). P5A0 had the highest values of circularity and solidity (Fig 2E and 2F). Circularity of most P10 and P15 significantly dropped compared with P5 in their respective treatment groups. P5 cells incubated with ALN at every concentration showed lower circularity than P5A0, whereas P10 and P15 cells treated with ALN at moderate concentrations showed reduction in circularity than P10A0 and P15A0, respectively (Fig 2E). Solidity showed a similar trend as circularity but in a lesser extent (Fig 2F).

Alteration of nuclear morphology in early, extended, and late passages under ALN-free and ALN conditions

Nuclei of the cells presented in bright blue color. The shape and size of P5A0 nuclei were homogenous and had oval shape (Fig 3Ai). Some nuclei of P10A0 and P15A0 appeared larger and less consistent (Fig 3Bi and 3Ci). Nuclear fragmentation was observed as shown in inset of Fig 3Ci. ALN treatment caused uneven nuclear shape and size of some nuclei. Nuclear fragmentation was also monitored (arrows) (Fig 3).

The numbers of nuclei represented the numbers of cells grown on the well plate. P5A0 displayed the highest value of nuclei. P10A0 and P15A0 nuclear numbers drastically declined compared with P5A0, implying slower growth rate in higher passages. The same pattern was seen in all ALN-treated groups except for A10 group. Every ALN concentration reduced the numbers of nuclei in P5 group, while moderate concentrations decreased nuclear numbers in P10 and P15 groups (Fig 4A).

In every ALN group, nuclear area and perimeter of P5 were smaller than those of P10 and P15. Nuclear area and perimeter of P5 were smaller in response to ALN at lower concentrations, whereas those of P10 and P15 changed at higher concentrations (Fig 4B and 4C).

AR values opposed to roundness values (Fig 4D and 4E). In A0-A0.5 groups, P10 and P15 had lower AR but higher roundness, suggesting rounder shape nuclei. On the other hand, AR and roundness of P10 and P15 in A5-A10 groups illustrated less circular shape nuclei compared with P5. DPSCs at P5 and P15 subjected to ALN treatment showed a reduction in AR and an increase in roundness (Fig 4D and 4E).

In general, circularity and solidity of P15 significantly reduced compared with those of P5 in every ALN group. Circularity and solidity of P15A10 were the lowest value in all condition (Fig 4F and 4G). These values were related to the irregular shape of some nuclei and nuclear breakage (Fig 3).

Comparison of cell adhesion in early, extended, and late passages under ALN-free and ALN conditions

Crystal violet-positive cells after 5 hours of cell seeding were shown in Figure 5. The numbers of cell adhesion in P5 were significantly greater than P10 and P15 in untreated and treated groups (Fig 6A). Cell area and perimeter of P15 were larger than those of P5 in ALN groups. DPSCs responded to ALN treatment by increased cell spreading (Fig 6B and 6C).

In A0-A0.5 groups, higher passages had lower AR compared with P5. In P5 group, treatment with ALN decreased AR (Fig 6D). Roundness had the opposite trend from AR (Fig 6E).

Cell circularity and solidity of P15 significantly decreased compared with those of P5 in every ALN condition. ALN treatment increased circularity and solidity of cells in P5 and P10 (Fig 6F and 6G).

Reduction of DPSC proliferative capability by replicative passaging and ALN addition

Figure 7 illustrates the proliferative capacity of DPSCs. Without ALN, cells in each passage had normal growth curve from day 1 to day 7. In A0 group, P5 cells maintained the optimal growth rate, whereas P15 had the slowest growth rate in all day tested. Compared with P5, P15 had the reduction rate approximately 50, 65, 70% for 1, 3, and 7 days, respectively (Fig 7). In ALN treatment groups, the proliferative rate of higher passages gradually reduced from P5. Low concentration of ALN did not affect cell proliferation. A5 and A10 significantly caused a considerable reduction in cell proliferation in every passage compared with their respective

passages. Long-term treatment and moderate dose of ALN almost abolished cell proliferation (Fig 7).

Effects of cell passages and ALN on total protein and ALP activity

The total protein of DPSCs cultured in OM for 7 days was extracted and measured. In general, P5 had higher total protein than P10 and P15 in each ALN group. P10 and P15 significantly had lower total protein compared with P5 in the presence of A5 and A10 (Fig 8A).

ALP activity was obtained from cell lysate and the release into the media. ALP of P10 significantly dropped compared with that of P5 in A0, A0.1, and A0.5 groups, while ALP of P10 increased compared with that of P5 in A10 groups (Fig 8B). ALN affected P5 cells by reducing ALP activity in a dose-dependent manner. ALP of P10A5 was enhanced compared with that of P10A0 (Fig 8B). No significant change was observed in ALP release in the media in all conditions (Fig 8C).

Effects of cell passages and ALN on gene expressions

Since DPSCs can differentiate into odontoblastic or osteoblastic cells, genes such as Col I, OC, BSP, DSPP, and DMP1 were examined. The data set were presented in 2 aspects: within the same ALN treatment group and within the same passage group. P15 had higher Col I gene expressions than P5 in A0.5, A5, and A10 groups. On the contrary, P15 and P10 had lower OC gene expressions than P5 in A0.5 and A10 groups, respectively. There was no change in BSP, DSPP, and DMP1 genes (Fig 9A). In P10 and P15, only A10 downregulated Col I gene expressions compared with A0. There was no change in other genes (Fig 9B).

Discussion

DPSCs are MSCs that have displayed multi-differentiation potential toward odontoblastic and osteogenic cells (Gronthos, Mankani et al. 2000, Mangano, Paino et al. 2011, Rodas-Junco and Villicana 2017, Sushmita, Chethan Kumar et al. 2019). These cells have become valuable alternative source of cells for the use in MSC-based therapies and studies varied from *in vitro* to *in vivo* (d'Aquino, De Rosa et al. 2009, Sushmita, Chethan Kumar et al. 2019). To obtain sufficient number of cells, continuously passaging primary cells can gradually lead to genetic and phenotypic changes, which could affect the use and the results in the experiments. The data from this study contributed that continuous cell expansion affected the experimental outcomes such as cell shape, activities as well as the response of cells to the ALN drug treatment (Summary shown in Figure 10).

After cell seeding, cells adhere to the substrate by making contact with the substrates, then spreading, and increasing their contact radius. The peak cell radius is observed at 18 h post-incubation (Fritsche, Luethen et al. 2013). The parameters that comprehensively and accurately reflect the process of cell attachment and spreading include cell number, cell area and area fraction, relative and accumulative frequency of cell area, cell circularity, perimeter, and Feret's diameter (Wang, Guo et al. 2021). We demonstrated for the first time that DPSC adhesion and its shape were influenced by cell passages and ALN addition. ALN has been shown to affect pre-osteoblast adhesion at high passages by decreasing cell adhering to the titanium surface (Lilakhunakon, Suwanpateeb et al. 2021). The quantitative assessment of cell shape helps elucidate the mechanism of initial cell adhesion, thus relatively estimating the direct interaction between cells and the substrate surface. Changes in cell shape by cell passages and ALN could

exhibit the alteration of DPSCs and the substrate surface interaction. Hence, the use of cells for regenerative medicine might be limited to lower passage especially at the presence of ALN.

Late passages of DPSCs had larger cell size, heterogenous uniform, and increase in cytoplasmic granularity as previously observed in DPSCs and another MSCs *in vitro* and *ex vivo* (Madeira, da Silva et al. 2012, Oja, Komulainen et al. 2018, Wang, Zhong et al. 2018, Mammoto, Torisawa et al. 2019). Cell size of bone marrow MSCs is visibly enlarged resulting in a 4.8-fold increase at P6–9 as compared to P1 (Oja, Komulainen et al. 2018). *Ex vivo* endothelial cells isolated from small blood vessels in adipose tissues show age-dependent increases in cell size (Mammoto, Torisawa et al. 2019). Furthermore, change in cell area is correlated with biochemical senescence markers such as p16^{INK4a} expression and senescence-associated β -galactosidase activity, suggesting a typical characteristic of aging cell (Oja, Komulainen et al. 2018). In this study, moderate dose of ALN also increased cell size of DPSCs. The replicative aging and ALN cause cell cycle arrest (Patntirapong, Korjai et al. 2021, Sanagawa, Hotta et al. 2022). An accumulation of the cells in the G2/M phase delay cells to enter into mitosis (Patntirapong, Korjai et al. 2021), thus increasing in the size of cells. Nuclear morphology, which is served as an indicator of cellular aging, shows a larger size in cultured aging cells and replicative senescent cells (Heckenbach, Mkrtchyan et al. 2022, Hartmann, Herling et al. 2023). Nuclear area of DPSCs demonstrated a larger size in serial expansion but was smaller when receiving ALN. Cell and nuclear area monitoring can be applied to many types of cell culture systems (Oja, Komulainen et al. 2018) as well as could be used for routine detection and prediction of mesenchymal cell aging and abnormality under an inverted microscope.

Cell shape change can be distinguished by the alteration of cell shape descriptors such as circularity and solidity parameters (Patntirapong 2023). Circularity and solidity values indicate

cell deformability and the presence of membrane protrusions including lamellipodia, filopodia, and blebbing. High values suggest lower cell deformability and fewer protrusions (Patntirapong 2023). The present data exhibited the reduction of cell circularity and solidity in continuous expansion and ALN treatment, implying higher cell deformability and more cell protrusions. Furthermore, nuclear shape of replicative senescent cells is irregular (Heckenbach, Mkrtchyan et al. 2022). Circularity and solidity values of nuclei together with nuclear irregular shape and nuclear breakage indicated abnormal nuclei after long-term subculture and/or obtaining moderate dose of ALN. Late passage cells with or without ALN treatment could drive the cells into cell death.

One of the properties of stem cells is an ability to proliferate. DPSC proliferation was passage dependent, which gradually reduced in increasing passage numbers. Although the rate of cell growth slowed down significantly compared with their early passage counterpart, late passage of DPSCs still proliferated. A reduction in the proliferative capacity of P15 did not yet reach the Hayflick limit but showed sign of replicative aging according to Ogrodnik (Ogrodnik 2021). The optimal proliferative capacity of DPSCs is reported at around P9 (Martin-Piedra, Garzon et al. 2013) and still have high cell viability, functionality, and intact membrane integrity up to P14 (Martin-Piedra, Garzon et al. 2014). The proliferation rate is reduced in late passage because the population doubling time in the late passage is longer than that in early passage (P9 at 3.42 days vs. P1 at 1.83 days) (Yu, He et al. 2010). Cells beyond P14 show a degree of cell membrane damage associated with metabolic impairment, suggesting a pre-apoptotic process (Martin-Piedra, Garzon et al. 2014). The decrease in proliferative ability *in vitro* was consistent with decreased proliferative ability in *ex vivo* aged donors. The stem cells derived from young donors (up to 25 years) maintain proliferative ability in all cell passages tested. Cells from the

aged group (up to 67 years) demonstrate a decline in proliferative ability (Bressan, Ferroni et al. 2012). Addition of ALN alone reduced cell proliferation in every cell passage tested. The presence of ALN stimuli might cause some cells to undergo premature programmed cell death earlier than others since ALN can trigger cell cycle arrest and cell damage (Patntirapong, Korjai et al. 2021). Combined effects of drug treatment and cell aging synergistically inhibited cell growth.

Differentiating DPSCs at different passages responded to stimuli differently. ALP is one of osteogenic/odontogenic markers. DPSCs at P5 and P10 responded in a different direction under ALN stimuli. P5 cells reacted to ALN treatment by reducing ALP levels in a dose-dependent manner, while P10 enhanced ALP level under ALN treatment. P10 had lower ALP activity in untreated and low dose ALN conditions but produced more ALP activity after receiving moderate dose ALN. DPSCs at P9 under OM present a higher ALP level than DPSC at P1, suggesting that a more advanced passage DPSCs are more inclined toward osteogenic/odontogenic lineage (Yu, He et al. 2010). This study did not show the same trend as previous report (Yu, He et al. 2010). Different responses of cells to cell passages and ALN were also observed at the gene levels. In ALN-free condition, osteogenic/odontogenic genes did not change by cell passage. Under ALN, Col I gene expressions increased, whereas OC gene expressions decreased in P15. However, Col I gene expressions were reduced by ALN. It has been shown that late passage of DPSCs exhibits lower osteogenic genes (Wang, Zhong et al. 2018). The passage used, genes tested, and the experimental settings might play a role in the different results. Since the results are inconsistent, more research may be essential.

MSC populations including DPSCs are able to expand *ex vivo/in vitro* for several passages. Nevertheless, cells cultured over a long period will eventually lose their fitness to the

point where cells are compromised and insufficient to support long-term use. Late passage underwent alteration from its original characteristics at earlier passages, as observed by changes in all parameter tested. These data were in accordance with previous reports (Martin-Piedra, Garzon et al. 2013, Martin-Piedra, Garzon et al. 2014, Wang, Zhong et al. 2018, Abdik, Avşar Abdik et al. 2019, Mammoto, Torisawa et al. 2019, Heckenbach, Mkrtchyan et al. 2022). It has been suggested that primary cells at a passage of less than 10 might be optimal for studies and tissue engineering purpose because these cells still have adequate qualities (Martin-Piedra, Garzon et al. 2013, Liao, He et al. 2014). Cells higher than P14 do not fulfill the quality control requirements and is recommended to be discarded (Martin-Piedra, Garzon et al. 2014) to minimize the risk of losing their stemness capacity (Lizier, Kerkis et al. 2012) and avoid the changes in phenotypic and genetic properties (Liao, He et al. 2014, Martin-Piedra, Garzon et al. 2014, Wang, Zhong et al. 2018) as well as to avoid susceptibility to the microbial contamination.

Replicative passaging demonstrates changes in the function of transporters in cells, thus altering cellular uptake of the substrate (Sanagawa, Hotta et al. 2022). Difference in cellular uptake could direct cell response to external factor differently and caused variable cell impairment in the presence of external factor. Based on the results, cells at lowest passage possible might be better suit for the study under the presence of external factor. Late passage would correspond to the studies of aged-related condition. The data in this study might provide guidance for the selection of appropriate and effective expanded DPSCs for distinctive study and therapeutic purposes.

Conclusion

Long-term subculture and ALN addition modulated DPSC behaviors at different extent *in vitro*. Without ALN condition, continuous cell expansion negatively affected number of cell adhesion, proliferation, and differentiation markers. Late passage cells were heterogeneity and displayed one of antagonistic aging markers, which is morphological changes of cells. Early, extended, and late passages responded to ALN differently in most aspects of cell behaviors. It is necessary to understand several biological aspects of these dental stem cell populations. This is to ensure the potential and the extent of their efficacy to guarantee the success in each scientific purpose.

Acknowledgements

The authors gratefully acknowledge Thammasat University Research Fund, Thammasat University, Contract No. TUFT 26/2566 for financial support of this work. This work was supported by Thammasat University Research Unit in Dental and Bone Substitute Biomaterials, Thammasat University. The authors also acknowledge Harikarn Mungpayabarn for technical assistance.

References

- Abdik, H., E. Avşar Abdik, S. Demirci, A. Doğan, D. Turan and F. Şahin (2019). "The effects of bisphosphonates on osteonecrosis of jaw bone: a stem cell perspective." Molecular Biology Reports **46**(1): 763-776.
- Awais, S., S. S. Balouch, N. Riaz and M. S. Choudhery (2020). "Human Dental Pulp Stem Cells Exhibit Osteogenic Differentiation Potential." Open Life Sci **15**: 229-236.

439 Bressan, E., L. Ferroni, C. Gardin, P. Pinton, E. Stellini, D. Botticelli, S. Sivoletta and B. Zavan
 440 (2012). "Donor age-related biological properties of human dental pulp stem cells change in
 441 nanostructured scaffolds." PLoS One **7**(11): e49146.

442 Chen, Y., X. Li, J. Wu, W. Lu, W. Xu and B. Wu (2021). "Dental pulp stem cells from human
 443 teeth with deep caries displayed an enhanced angiogenesis potential in vitro." J Dent Sci **16**(1):
 444 318-326.

445 d'Aquino, R., A. De Rosa, V. Lanza, V. Tirino, L. Laino, A. Graziano, V. Desiderio, G. Laino and
 446 G. Papaccio (2009). "Human mandible bone defect repair by the grafting of dental pulp
 447 stem/progenitor cells and collagen sponge biocomplexes." Eur Cell Mater **18**: 75-83.

448 Fritsche, A., F. Luethen, U. Lembke, C. Zietz, J. Rychly, W. Mittelmeier and R. Bader (2013).
 449 "Time-dependent adhesive interaction of osteoblastic cells with polished titanium alloyed implant
 450 surfaces." J Appl Biomater Funct Mater **11**(1): e1-8.

451 Gao, Y., X. You, Y. Liu, F. Gao, Y. Zhang, J. Yang and C. Yang (2020). "Induction of autophagy
 452 protects human dental pulp cells from lipopolysaccharide-induced pyroptotic cell death." Exp Ther
 453 Med **19**(3): 2202-2210.

454 Gronthos, S., M. Mankani, J. Brahimi, P. G. Robey and S. Shi (2000). "Postnatal human dental
 455 pulp stem cells (DPSCs) in vitro and in vivo." Proc Natl Acad Sci U S A **97**(25): 13625-13630.

456 Grotheer, V., N. Skrynecki, L. Oezel, J. Windolf and J. Grassmann (2021). "Osteogenic
 457 differentiation of human mesenchymal stromal cells and fibroblasts differs depending on tissue
 458 origin and replicative senescence." Sci Rep **11**(1): 11968.

459 Hart, M. L., J. C. Lauer, M. Selig, M. Hanak, B. Walters and B. Rolaufts (2017). "Shaping the cell
 460 and the future: Recent advancements in biophysical aspects relevant to regenerative medicine." J
 461 Funct Morphol Kinesiol **3**(2): 1-16.

462 Hartmann, C., L. Herling, A. Hartmann, V. Kockritz, G. Fuellen, M. Walter and A. Hermann
 463 (2023). "Systematic estimation of biological age of in vitro cell culture systems by an age-
 464 associated marker panel." Front Aging **4**: 1129107.

465 Hayflick, L. and P. S. Moorhead (1961). "The serial cultivation of human diploid cell strains."
 466 Experimental Cell Research **25**(3): 585-621.

467 Heckenbach, I., G. V. Mkrtchyan, M. B. Ezra, D. Bakula, J. S. Madsen, M. H. Nielsen, D. Oro, B.
 468 Osborne, A. J. Covarrubias, M. L. Idda, M. Gorospe, L. Mortensen, E. Verdin, R. Westendorp and
 469 M. Scheibye-Knudsen (2022). "Nuclear morphology is a deep learning biomarker of cellular
 470 senescence." Nat Aging **2**(8): 742-755.

471 Huang, G. T., S. Gronthos and S. Shi (2009). "Mesenchymal stem cells derived from dental tissues
 472 vs. those from other sources: their biology and role in regenerative medicine." J Dent Res **88**(9):
 473 792-806.

474 Kogo, Y., C. Seto, Y. Totani, M. Mochizuki, T. Nakahara, K. Oka, T. Yoshioka and E. Ito (2020).
 475 "Rapid differentiation of human dental pulp stem cells to neuron-like cells by high
 476 K⁺ stimulation." Biophysics and Physicobiology **17**: 132-139.

477 Liao, H., H. He, Y. Chen, F. Zeng, J. Huang, L. Wu and Y. Chen (2014). "Effects of long-term
 478 serial cell passaging on cell spreading, migration, and cell-surface ultrastructures of cultured
 479 vascular endothelial cells." Cytotechnology **66**(2): 229-238.

480 Lilakhunakon, C., J. Suwanpateeb and S. Patntirapong (2021). "Inhibitory Effects of Alendronate
 481 on Adhesion and Viability of Preosteoblast Cells on Titanium Discs." Eur J Dent **15**(3): 502-508.

482 Lizier, N. F., A. Kerkis, C. M. Gomes, J. Hebling, C. F. Oliveira, A. I. Caplan and I. Kerkis (2012).
 483 "Scaling-up of dental pulp stem cells isolated from multiple niches." PLoS One **7**(6): e39885.

484 Madeira, A., C. L. da Silva, F. dos Santos, E. Camafeita, J. M. Cabral and I. Sa-Correia (2012).
 485 "Human mesenchymal stem cell expression program upon extended ex-vivo cultivation, as
 486 revealed by 2-DE-based quantitative proteomics." PLoS One 7(8): e43523.

487 Mammoto, T., Y. S. Torisawa, M. Muyleart, K. Hendee, C. Anugwom, D. Gutterman and A.
 488 Mammoto (2019). "Effects of age-dependent changes in cell size on endothelial cell proliferation
 489 and senescence through YAP1." Aging (Albany NY) 11(17): 7051-7069.

490 Mangano, C., F. Paino, R. d'Aquino, A. De Rosa, G. Iezzi, A. Piattelli, L. Laino, T. Mitsiadis, V.
 491 Desiderio, F. Mangano, G. Papaccio and V. Tirino (2011). "Human dental pulp stem cells hook
 492 into biocoral scaffold forming an engineered biocomplex." PLoS One 6(4): e18721.

493 Martin-Piedra, M. A., I. Garzon, A. C. Oliveira, C. A. Alfonso-Rodriguez, V. Carriel, G. Scionti
 494 and M. Alaminos (2014). "Cell viability and proliferation capability of long-term human dental
 495 pulp stem cell cultures." Cytotherapy 16(2): 266-277.

496 Martin-Piedra, M. A., I. Garzon, A. C. Oliveira, C. A. Alfonso-Rodriguez, M. C. Sanchez-
 497 Quevedo, A. Campos and M. Alaminos (2013). "Average cell viability levels of human dental pulp
 498 stem cells: an accurate combinatorial index for quality control in tissue engineering." Cytotherapy
 499 15(4): 507-518.

500 Ogrodnik, M. (2021). "Cellular aging beyond cellular senescence: Markers of senescence prior to
 501 cell cycle arrest in vitro and in vivo." Aging Cell 20(4): e13338.

502 Oja, S., P. Komulainen, A. Penttila, J. Nystedt and M. Korhonen (2018). "Automated image
 503 analysis detects aging in clinical-grade mesenchymal stromal cell cultures." Stem Cell Res Ther
 504 9(1): 6.

505 Pasqualato, A., V. Lei, A. Cucina, S. Dinicola, F. D'Anselmi, S. Proietti, M. G. Masiello, A.
 506 Palombo and M. Bizzarri (2013). "Shape in migration: quantitative image analysis of migrating
 507 chemoresistant HCT-8 colon cancer cells." Cell Adh Migr **7**(5): 450-459.
 508 Patntirapong, S. (2023). "Cell Shape Description as a Tool for Assessing Cell Change after Drug
 509 Treatments." Science & Technology Asia **28**(3): 231-238.
 510 Patntirapong, S., C. Chanruangvanit, K. Lavanrattanakul and Y. Satravaha (2021). "Assessment
 511 of bisphosphonate treated-osteoblast behaviors by conventional assays and a simple digital image
 512 analysis." Acta Histochem **123**(1): 151659.
 513 Patntirapong, S., P. Charoensukpatana and T. Thaksinawong (2022). "Changes in Cell Size and
 514 Dimension Characterized by Crystal Violet Staining and Simple ImageJ Analysis." Journal of
 515 International Dental and Medical Research **15**(1).
 516 Patntirapong, S., N. Korjai, M. Matchimapiro, P. Sungkaruk and Y. Suthamporn (2021).
 517 "Geranylgeraniol reverses alendronate-induced MC3T3 cell cytotoxicity and alteration of
 518 osteoblast function via cell cytoskeletal maintenance." J Oral Pathol Med **50**(2): 191-199.
 519 Patntirapong, S., W. Singhatanadgit and S. Arphavasin (2014). "Alendronate-induced atypical
 520 bone fracture: evidence that the drug inhibits osteogenesis." J Clin Pharm Ther **39**(4): 349-353.
 521 Rodas-Junco, B. A. and C. Villicana (2017). "Dental Pulp Stem Cells: Current Advances in
 522 Isolation, Expansion and Preservation." Tissue Eng Regen Med **14**(4): 333-347.
 523 Sanagawa, A., Y. Hotta, R. Sezaki, N. Tomita, T. Kataoka, Y. Furukawa-Hibi and K. Kimura
 524 (2022). "Effect of Replicative Senescence on the Expression and Function of Transporters in
 525 Human Proximal Renal Tubular Epithelial Cells." Biological and Pharmaceutical Bulletin **45**(11):
 526 1636-1643.

527 Simon, A., T. Cohen-Bouhacina, M. C. Porte, J. P. Aime, J. Amedee, R. Bareille and C. Baquey
 528 (2003). "Characterization of dynamic cellular adhesion of osteoblasts using atomic force
 529 microscopy." Cytometry A **54**(1): 36-47.

530 Sushmita, V. P., J. S. Chethan Kumar, C. Hegde and B. G. S. Kurkalli (2019). "Interaction of
 531 dental pulp stem cells in bone regeneration on titanium implant. An in vitro study." Journal of
 532 Osseointegration **11**(4): 553-560.

533 Wang, H., Q. Zhong, T. Yang, Y. Qi, M. Fu, X. Yang, L. Qiao, Q. Ling, S. Liu and Y. Zhao (2018).
 534 "Comparative characterization of SHED and DPSCs during extended cultivation in vitro." Mol
 535 Med Rep **17**(5): 6551-6559.

536 Wang, Z., Y. Guo and P. Zhang (2021). "A rapid quantitation of cell attachment and spreading
 537 based on digital image analysis: Application for cell affinity and compatibility assessment of
 538 synthetic polymers." Mater Sci Eng C Mater Biol Appl **128**: 112267.

539 Yan, M., O. A. Nada, L. L. Fu, D. Z. Li, H. C. Feng, L. M. Chen, M. Gosau, R. E. Friedrich and
 540 R. Smeets (2022). "A comparative study on the secretion of various cytokines by pulp stem cells
 541 at different passages and their neurogenic potential." Biomed Pap Med Fac Univ Palacky Olomouc
 542 Czech Repub **166**(2): 161-167.

543 Yang, Y. K., C. R. Ogando, C. Wang See, T. Y. Chang and G. A. Barabino (2018). "Changes in
 544 phenotype and differentiation potential of human mesenchymal stem cells aging in vitro." Stem
 545 Cell Res Ther **9**(1): 131.

546 Yu, J., H. He, C. Tang, G. Zhang, Y. Li, R. Wang, J. Shi and Y. Jin (2010). "Differentiation
 547 potential of STRO-1+ dental pulp stem cells changes during cell passaging." BMC Cell Biol **11**:
 548 32.

549

Conflict of interest

The authors declare that they have no conflict of interest.

Figure legends

Fig 1 Dental pulp stem cell morphology. Every DPSC passage appeared in violet color except the image of P1 cells was shown in bright field. (A) P5 (B) P10 (C) P15 (D) P1. (i) A0 (ii) A0.1 (iii) A0.5 (iv) A5 (v) A10. Bar = 200 μm

Fig 2 Measurement of cell morphology. (A) Cell area (μm^2) (B) Cell perimeter (μm) (C) Aspect Ratio (D) Roundness (E) Circularity (F) Solidity.

Fig 3 Nuclear morphology of dental pulp stem cells. Nuclei stained in bright blue color. (A) P5 (B) P10 (C) P15. (i) A0 (ii) A0.1 (iii) A0.5 (iv) A5 (v) A10. Dashed box presents magnified view of fragmented nucleus. Arrows indicate nuclear fragmentation. Bar = 100 μm

Fig 4 Measurement of nuclear morphology. (A) Number of nuclei (B) Cell area (μm^2) (C) Cell perimeter (μm) (D) Aspect Ratio (E) Roundness (F) Circularity (G) Solidity.

Fig 5. Cell adhesion. (A) P5 (B) P10 (C) P15. (i) A0 (ii) A0.1 (iii) A0.5 (iv) A5 (v) A10. Bar = 200 μm

Fig 6 Measurement of cell adhesion. (A) Number of cells (B) Cell area (μm^2) (C) Cell perimeter (μm) (D) Aspect Ratio (E) Roundness (F) Circularity (G) Solidity.

Fig 7 Cell proliferation. DPSCs at early, extended, and late passages were grown in the absence or presence of ALN for 1, 3, and 7 days. Cells in every passage were able to proliferate at a different rate. Continuous passaging and ALN drastically reduced cell proliferation.

Fig 8 Total protein and alkaline phosphatase activity. (A) Total protein of differentiating dental pulp cells (B) ALP in cells (C) ALP released in the media.

573 **Fig 9** Gene expressions. (A) Genes were expressed and compared within ALN treatment groups.
574 (B) Genes were expressed and compared within the passage groups.

575 **Fig 10** A schematic diagram summarizes the effects of continuous cell passaging and ALN on
576 cell morphology, nuclear morphology, cell adhesion, cell proliferation, and ALP activity. Cell
577 morphology presented in violet color, while nuclear morphology presented in blue color. Cell
578 adhesion and cell proliferation were reduced by continuous cell passaging and ALN (Triangular).
579 ALP activity showed no particular pattern (Rectangle).

Figure 1

Figure 1

Dental pulp stem cell morphology. Every DPSC passage appeared in violet color except the image of P1 cells was shown in bright field. (A) P5 (B) P10 (C) P15 (D) P1. (i) A0 (ii) A0.1 (iii) A0.5 (iv) A5 (v) A10. Bar = 200 μ m

Figure 1

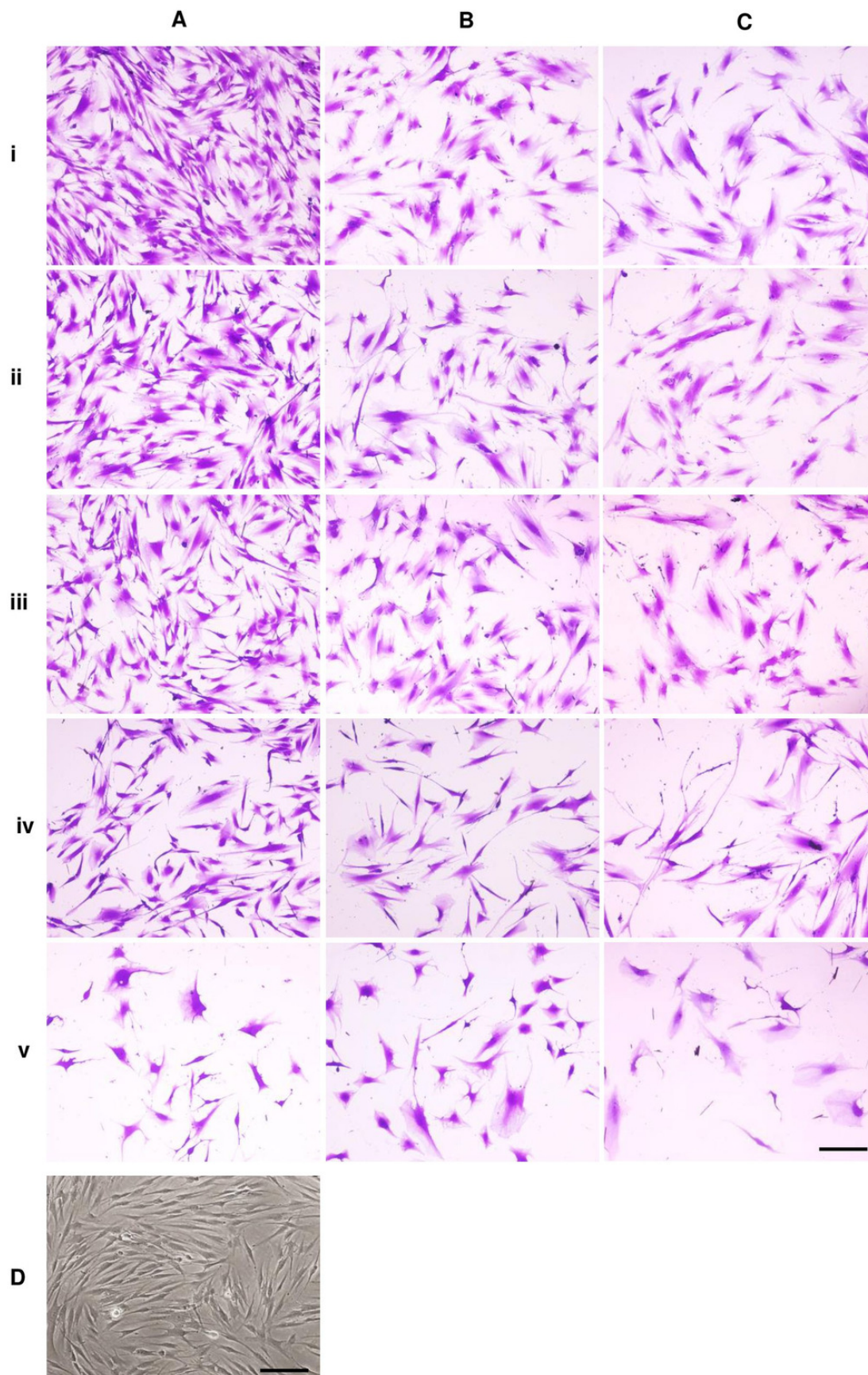


Figure 2

Figure 2

Measurement of cell morphology. (A) Cell area (μm^2) (B) Cell perimeter (μm) (C) Aspect Ratio (D) Roundness (E) Circularity (F) Solidity.

Figure 2

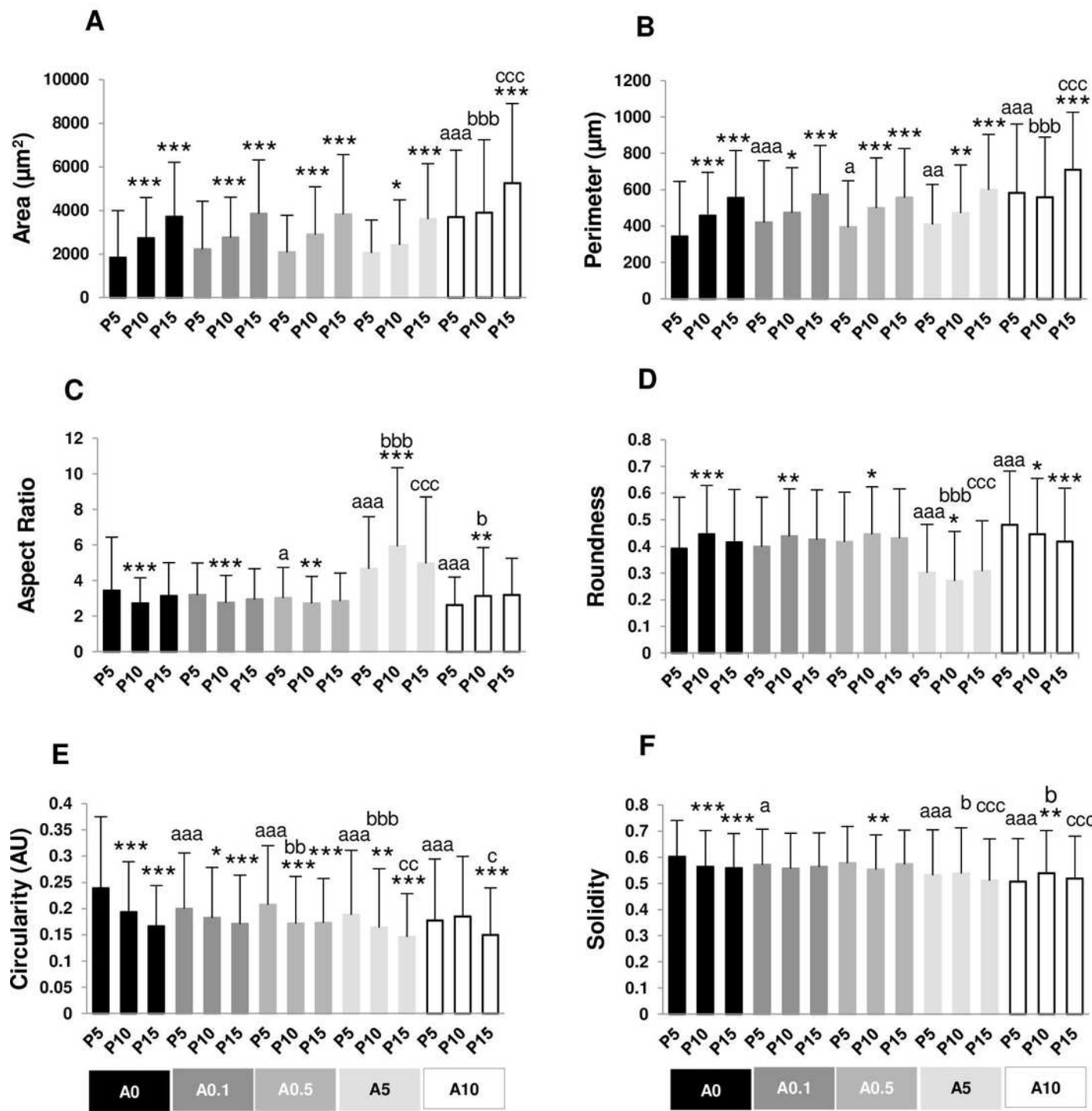


Figure 3

Figure 3

Nuclear morphology of dental pulp stem cells. Nuclei stained in bright blue color. (A) P5 (B) P10 (C) P15. (i) A0 (ii) A0.1 (iii) A0.5 (iv) A5 (v) A10. Dashed box presents magnified view of fragmented nucleus. Arrows indicate nuclear fragmentation. Bar = 100 μ m

Figure 3

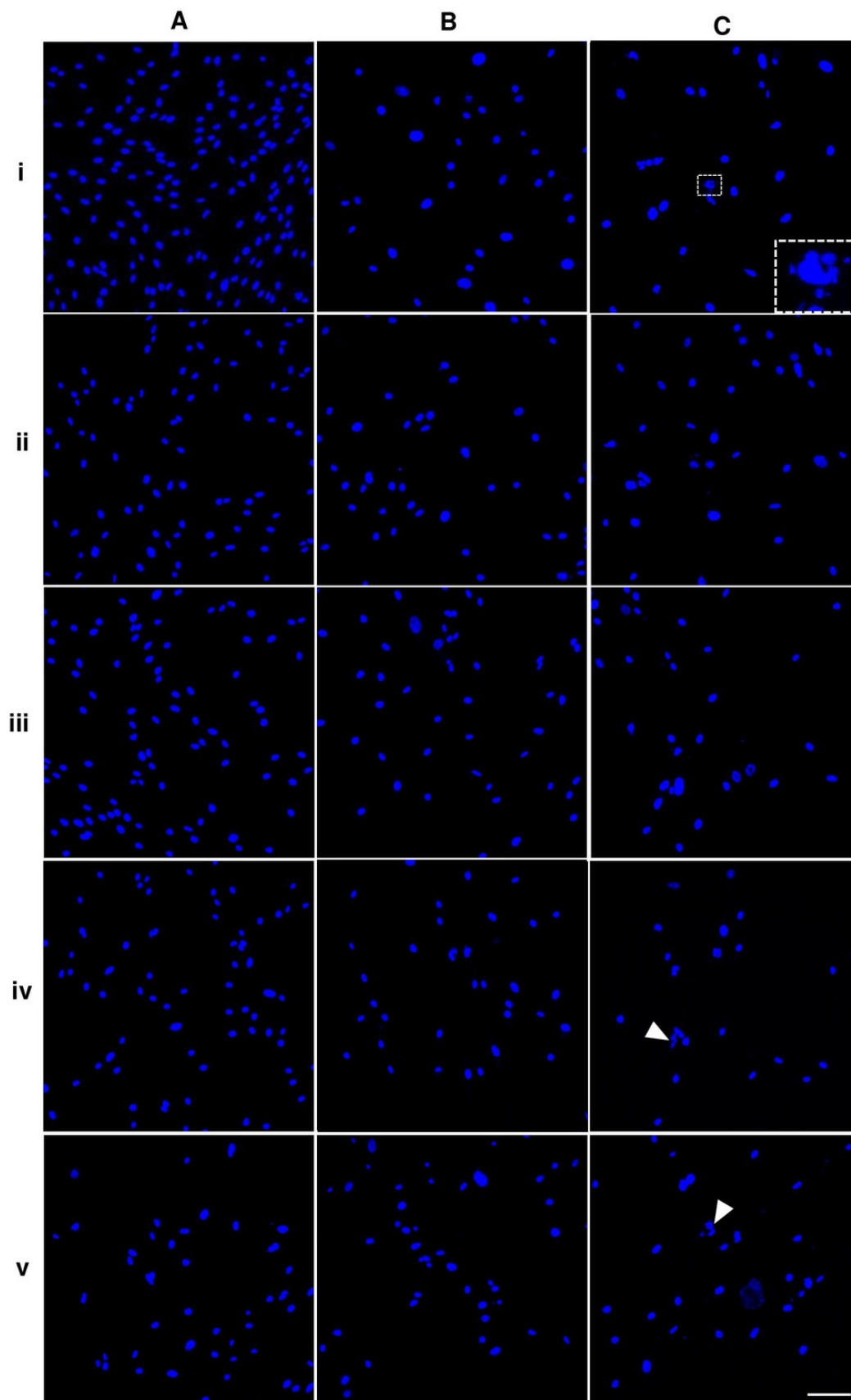


Figure 4

Figure 4

Measurement of nuclear morphology. (A) Number of nuclei (B) Cell area (μm^2) (C) Cell perimeter (μm) (D) Aspect Ratio (E) Roundness (F) Circularity (G) Solidity.

Figure 4

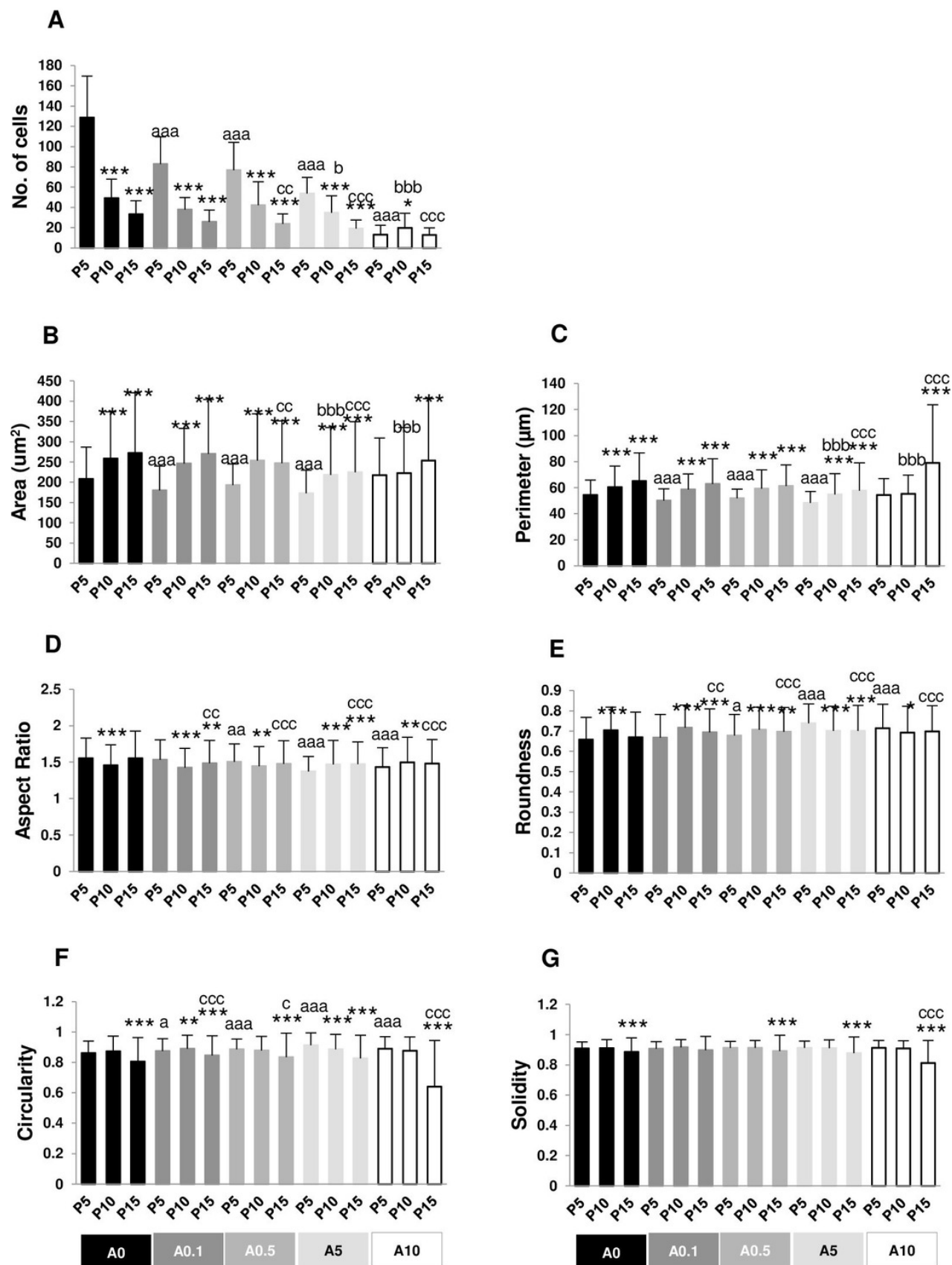


Figure 5

Figure 5

Cell adhesion. (A) P5 (B) P10 (C) P15. (i) A0 (ii) A0.1 (iii) A0.5 (iv) A5 (v) A10. Bar = 200 μm

Figure 5

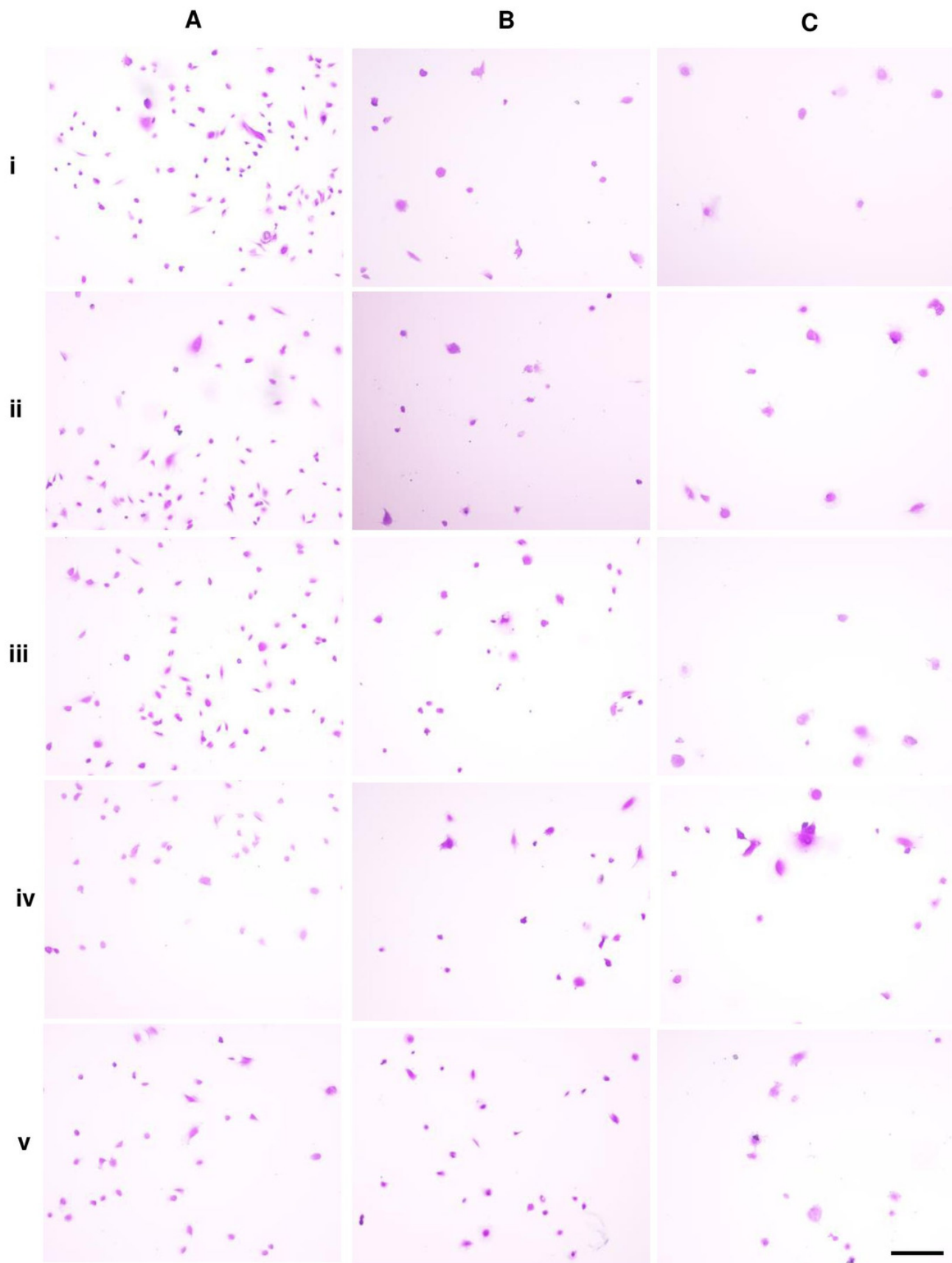


Figure 6

Figure 6

Measurement of cell adhesion. (A) Number of cells (B) Cell area (μm^2) (C) Cell perimeter (μm) (D) Aspect Ratio (E) Roundness (F) Circularity (G) Solidity.

Figure 6

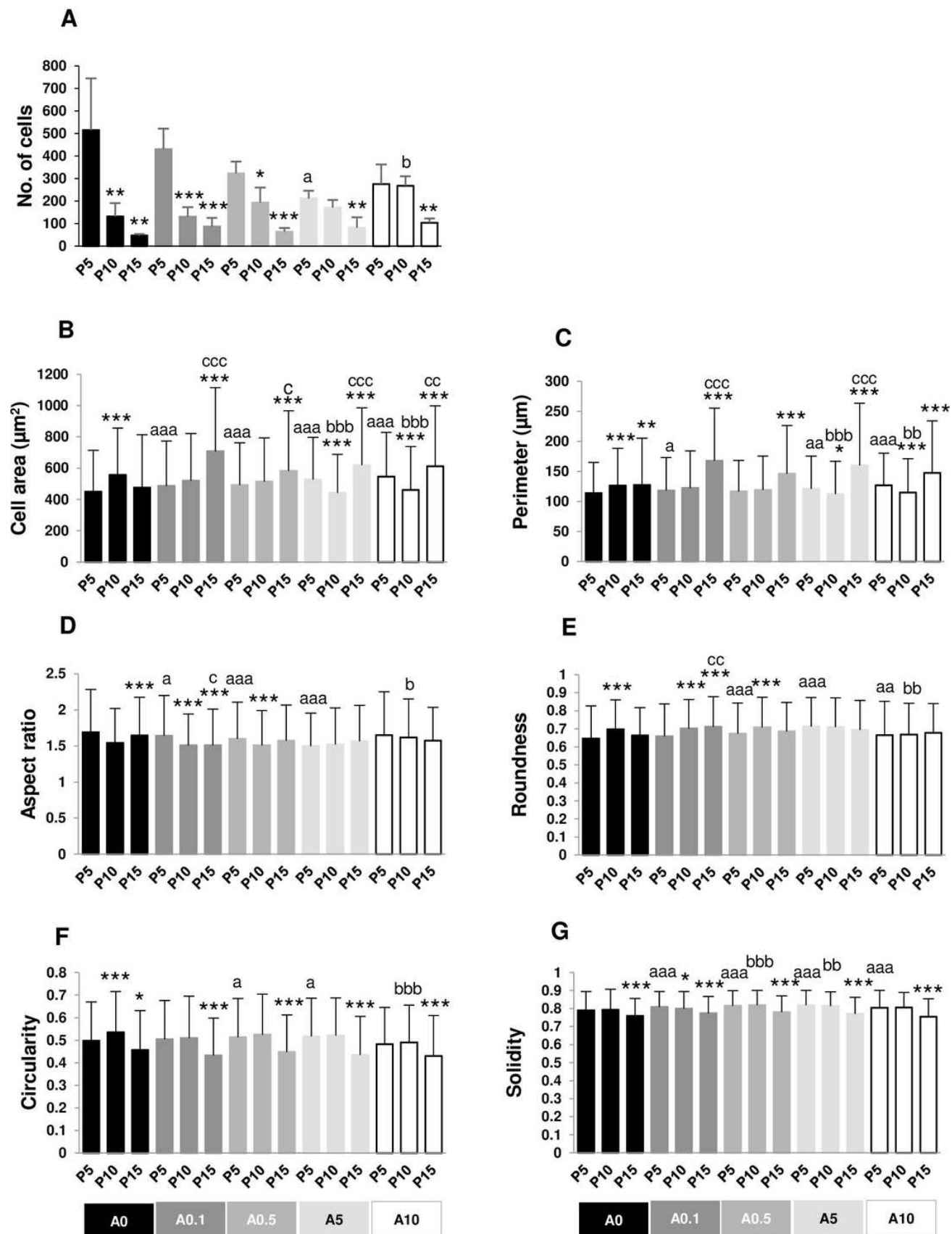


Figure 7

Figure 7

Cell proliferation. DPSCs at early, extended, and late passages were grown in the absence or presence of ALN for 1, 3, and 7 days. Cells in every passage were able to proliferate at a different rate. Continuous passaging and ALN drastically reduced cell proliferation.

Figure 7

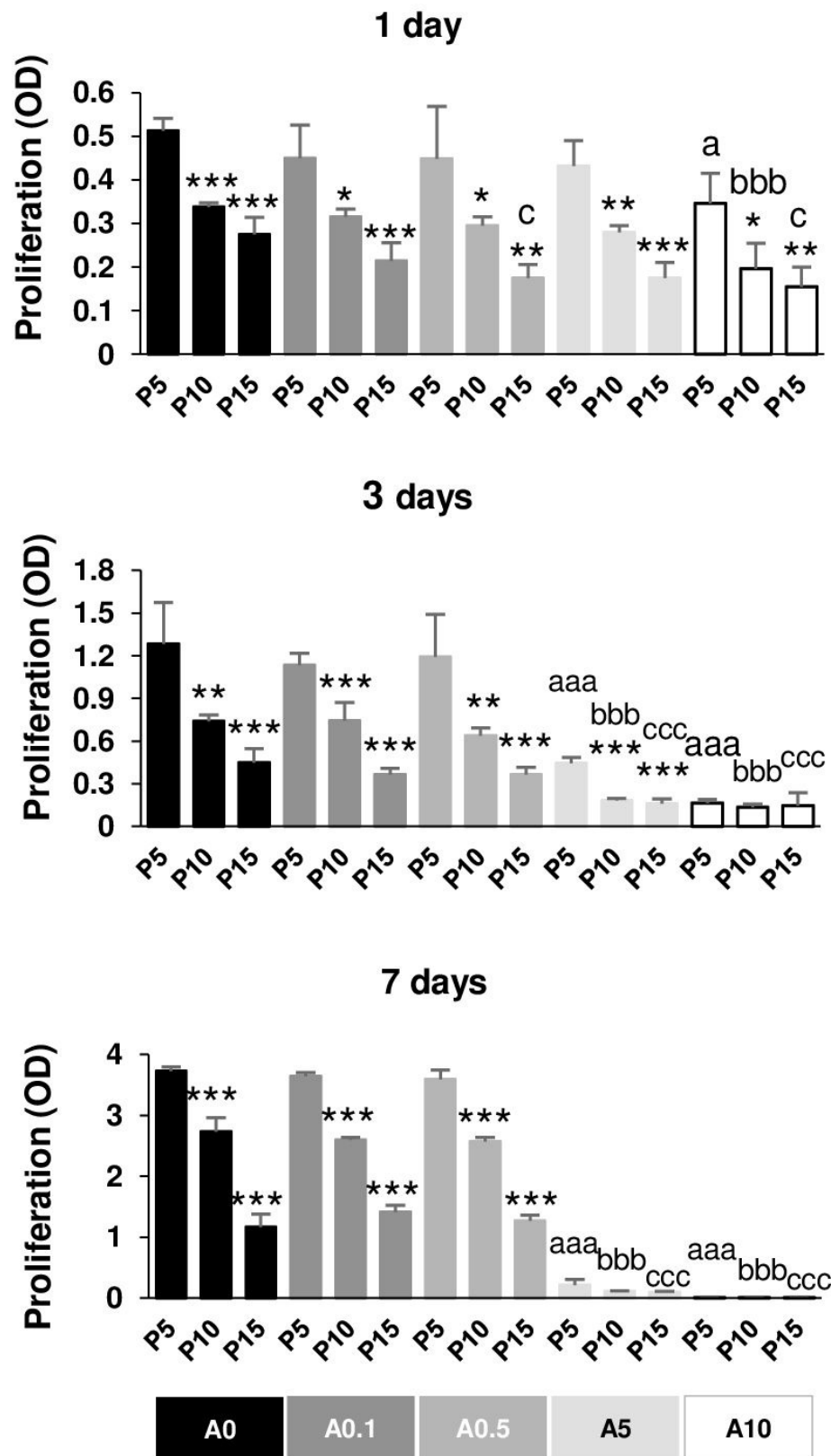


Figure 8

Figure 8

Total protein and alkaline phosphatase activity. (A) Total protein of differentiating dental pulp cells (B) ALP in cells (C) ALP released in the media.

Figure 8

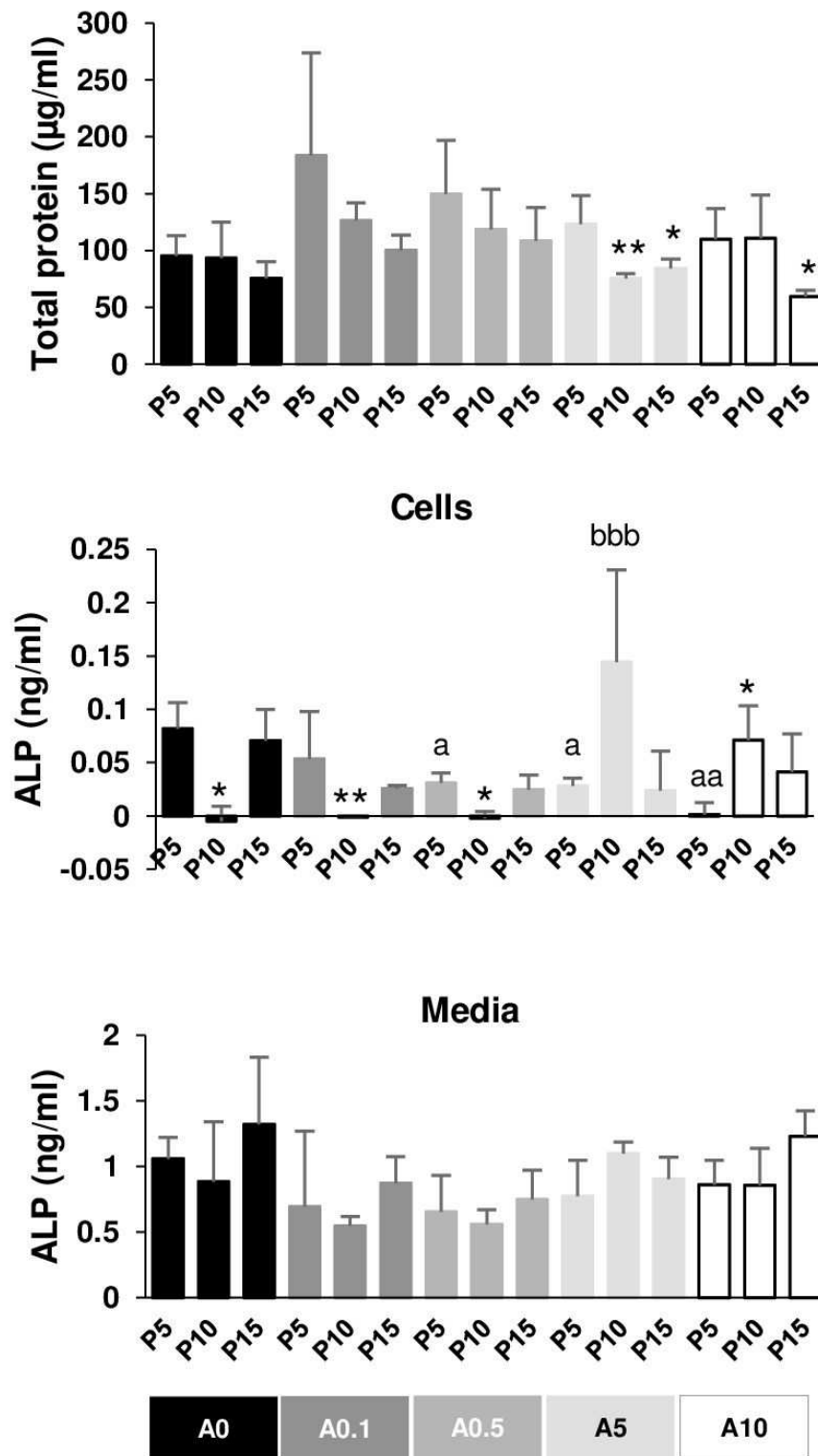


Figure 9

Figure 9

Gene expressions. (A) Genes were expressed and compared within ALN treatment groups.
(B) Genes were expressed and compared within the passage groups.

Fig 9

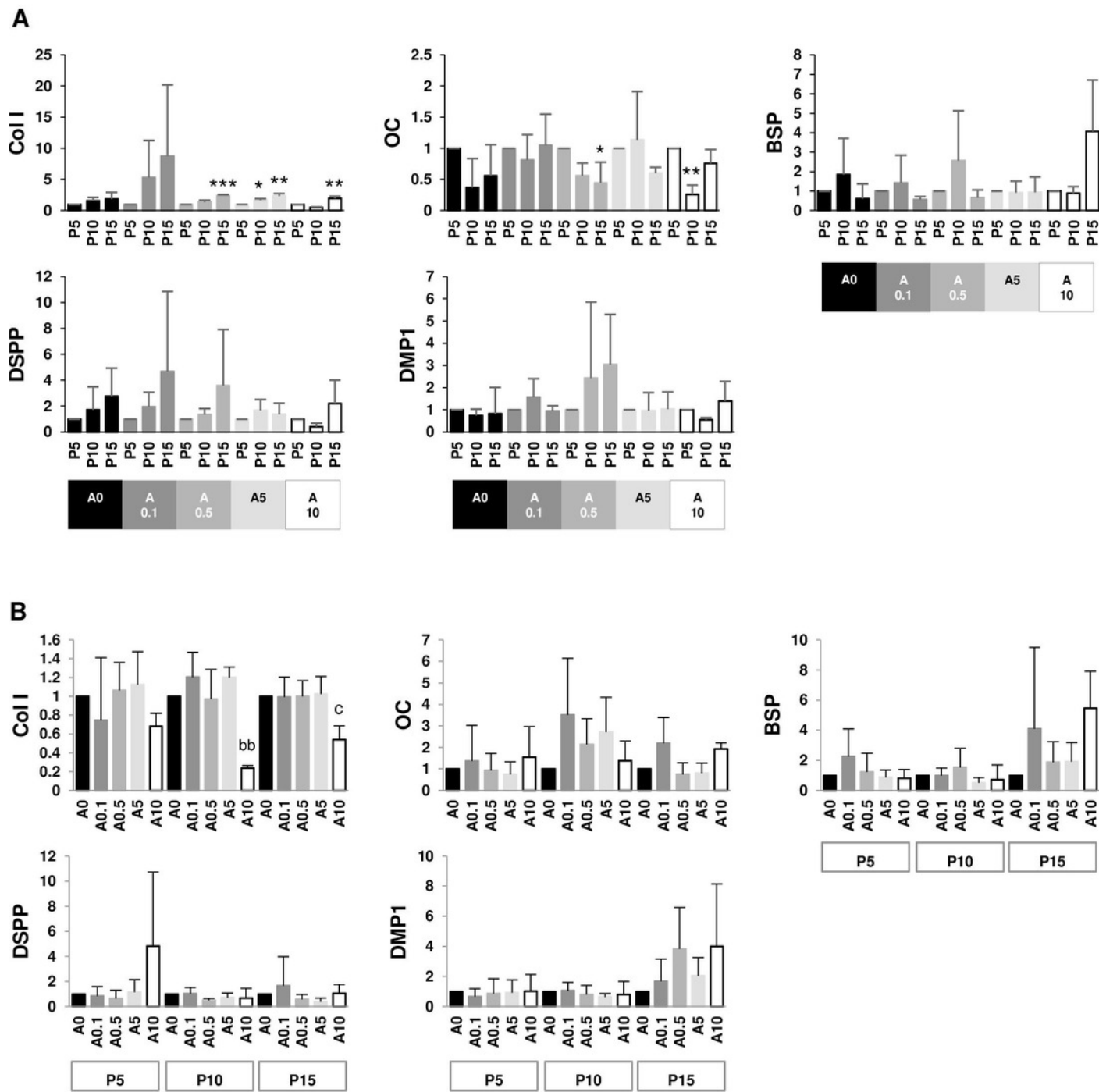


Figure 10

Figure 10

A schematic diagram summarizes the effects of continuous cell passaging and ALN on cell morphology, nuclear morphology, cell adhesion, cell proliferation, and ALP activity. Cell morphology presented in violet color, while nuclear morphology presented in blue color. Cell adhesion and cell proliferation were reduced by continuous cell passaging and ALN (Triangular). ALP activity showed no particular pattern (Rectangle).

Fig 10

